Clays and Clay Minerals, Vol. 46, No. 3, 232–239, 1998.

MOLECULAR SIMULATIONS OF MONTMORILLONITE INTERCALATED WITH ALUMINUM COMPLEX CATIONS. PART I: INTERCALATION WITH $[Al_{13}O_4(OH)_{24+x}(H_2O)_{12-x}]^{(7-x)+}$

P. ČAPKOVÁ,[1,2] R. A. J. DRIESSEN,[1] M. NUMAN,[1] H. SCHENK,[1] Z. WEISS[3] AND Z. KLIKA[3]

[1] Laboratory of Crystallography, AIMS, University of Amsterdam, Nieuwe Achtergracht 166, 1018 WV Amsterdam, The Netherlands

[2] Faculty of Mathematics and Physics, Charles University Prague, Ke Karlovu 5, 121 16 Prague, Czech Republic

[3] Central Analytical Laboratory, Technical University Ostrava, 70833 Ostrava, Czech Republic

Abstract—The structure of montmorillonite intercalated with $[Al_{13}O_4(OH)_{24+x}(H_2O)_{12-x}]^{(7-x)+}$ cations ($Al_{13}^{(7-x)+}$ for short), where x = 0, 2 and 4, has been studied using the Cerius^2 modeling environment. The Crystal Packer module used in the present study takes into account only the nonbonded interactions between the silicate layer and the Keggin cations. Minimization of the total sublimation energy led to the following conclusions: the structure of the interlayer (that is, the orientation of Keggin cations and the basal spacing) depends on the charge of cations (that is, on the degree of hydrolysis, x). The values of basal spacings in the range 19.38–20.27 Å have been obtained, depending on the charge and arrangement of cations in the interlayer. The dominating contribution to the total sublimation energy comes from the electrostatic interactions. Translations of $Al_{13}^{(7-x)+}$ cations along the 2:1 layers give only small fluctuations of the total sublimation energy and basal spacings. No preference for the position of $Al_{13}^{(7-x)+}$ cations in the interlayer of montmorillonite was found during translation along the 2:1 layers. This result confirmed the inhomogeneous distribution of cations in the interlayer and turbostratic stacking of layers.

Key Words—Al-Cations, Intercalation, Molecular Simulation, Montmorillonite, Structure.

INTRODUCTION

The numerous practical applications suggested for intercalated (pillared) clays require detailed structure analysis focused to the size, shape and distribution of pores in the interlayer space. Structural investigation using diffraction methods is extremely difficult in the case of intercalated clays. Structures of intercalated clays, especially those of the smectite group, exhibit turbostratic arrangement of layers, inhomogeneity in *d*-spacing, high amplitudes of thermal motion perpendicular to silicate layers and small particle size. As a result of all these effects, the powder X-ray diffraction (XRD) pattern exhibits only the first two 00*l* reflections and 2-dimensional *hk*-diffraction bands. Therefore, XRD analysis alone cannot provide all the parameters necessary for detailed analysis of structure porosity. In such a case, the molecular simulations represent a very powerful tool to study the structure and property relations.

Molecular simulations predict crystal structure and properties using energy minimization. The crystal energy in molecular simulations is described by the empirical force field. The potential energy for an arbitrary geometry of a molecule or crystal structure is expressed as a superposition of valence (or bonded) interactions that depend on the given bonding geometry and nonbonded interactions (van der Waals (VDW), coulombic (COUL) and hydrogen bond (HB), depending only on the distance between the atoms. Valence interactions consist of bond stretch, bond-angle bend, dihedral angle torsion and inversion terms (Mayo et al. 1990). The strategy of modeling (that is, the choice of force field, initial model and minimization conditions) depends on a given problem.

The so-called Keggin (or Al_{13}) cation $[Al_{13}O_4(OH)_{24}(H_2O)_{12}]^{7+}$ has been widely accepted as the pillaring species (Pinnavaia et al. 1984; Plee et al. 1985; Shoonheydt et al. 1994). Figueras (1988) showed that the amount of Al sorbed during an ion exchange reaction usually exceeds that necessary for charge neutralization with a Keggin cation. This may lead to 2 possible conclusions: 1) The Keggin cations are partially hydrolyzed and, consequently, carry a lower charge according to the formula $[Al_{13}O_4(OH)_{24+x}(H_2O)_{12-x}]^{(7-x)+}$, denoted as $Al_{13}^{(7-x)+}$. 2) The Keggin cations are not the only pillaring species. In the present work we analyzed both alternatives, investigating the effect of intercalation of Keggin cations (Part I) as well as 6-member rings of hydroxy-aluminum cations (Part II) on the structure of montmorillonite using the Crystal Packer module of the Cerius^2 modeling environment.

STRATEGY OF MODELING

Crystal Packer is a computational module in the Cerius^2 modeling environment that assists in the estimation of the total sublimation energy and packing of molecular crystals. Crystal Packer is based on the Dreiding II force field developed by Mayo et al. (1990). The primary advantage of the Dreiding force

field is its robustness. It is a good, all-purpose force field that can be used for structure predictions for a large number of organic and inorganic structures. Its parameterization is based on both *ab initio* and experimental data. Energy calculations in Crystal Packer take into account the nonbond terms only: VDW, COUL, HB, internal rotations and hydrostatic pressure. The asymmetric unit of the crystal structure is divided into fragment-based rigid units. Nonbond (VDW, COUL, HB) energies are calculated between the rigid units. During energy minimization, the rigid units can be translated and rotated and the unit cell parameters varied.

Model with the Ideal Keggin Cation $[Al_{13}O_4(OH)_{24}(H_2O)_{12}]^{7+}$

The initial model of the 2:1 layer of montmorillonite (MMT) was built using the PLUVA 2.3 program developed in the Laboratory for Crystallography, University of Amsterdam (Driessen et al. 1988), and structural data for montmorillonite given by Tsipursky and Drits (1984) (space group *C*2/m). The unit cell parameters, according to Mering and Oberlin (1967), have been used to define the planar unit cell dimensions: a = 5.208 Å and b = 9.02 Å. The 2:1 layers were removed to the distance 21 Å, allowing placement of the Al_{13}-cation into the interlayer space of the initial model. The structure of the Al_{13}-cation was built according to Johansson (1960). Supposing the composition of the 2:1 layer to be $(Al_{3.1}Mg_{0.9})Si_8O_{20}(OH)_4$, and taking into account the size and charge of the Al_{13}-cation, we created the supercell containing 8 unit cells as described above. The concentration of Keggin cations in the interlayer space is ruled by the negative charge density in the 2:1 silicate layer. In the supercell consisting of 8 MMT cells, only 7 MMT cells can contain the Al $\rightarrow$ Mg substitution, according to the present layer composition; that is, this supercell (8-MMT) containing one Al_{13}^{7+} cation carries the layer charge (7−). Consequently, the concentration of charge balancing cations is 0.125 Al_{13}^{7+} cations per MMT unit cell, corresponding to the concentration of interlayer aluminum 1.63 Al atoms per MMT unit cell. This concentration is in agreement with the data published by Malla and Komareni (1993) and Sterte (1991), where the aluminum contents in the interlayer space after intercalation were 1.66 and 1.74 Al atoms per MMT unit cell, respectively.

The following 8-MMT supercell parameters A, B, C, α, β, γ were set up for the initial model:

$A = 4a$ = 20.83 Å, fixed during energy minimization (a is the parameter of the original MMT cell),
$B = 2b$ = 18.04 Å, fixed (b is the parameter of the original MMT cell),
C, variable (C-axis perpendicular to sheets), α and β, variable, γ = 90°, fixed.

Models with Hydrolyzed Keggin Cations

Two different degrees of hydrolysis of Keggin cation $Al_{13}^{(7-x)+}$ have been considered: x = 2, 4. In this case, the models were built with respect to the 2 requirements: 1) to keep the charge neutrality of the model and 2) to keep the composition and, consequently, the charge density of the silicate layer.

The supercell with 2 Al_{13}^{5+} cations consists of 10 MMT unit cells. In this case, 1 MMT unit cell contains 1 Mg atom, corresponding to the layer composition $(Al_3Mg_1)Si_8O_{20}(OH)_4$. It follows that the 10-MMT supercell carries the layer charge (10−), balanced with 2 Al_{13}^{5+} cations. That means the concentration of cations is 0.2 per MMT cell; that is, the interlayer aluminum content after intercalation is 2.6 Al atoms per MMT unit cell. This concentration nearly corresponds to data published by Occelli and Rennard (1988) and Tichit et al. (1988), where the aluminum contents in the interlayer space after intercalation were 2.32 and 2.86 Al atoms per MMT unit cell, respectively.

The 10-MMT supercell parameters in the initial model were:

$A = 5a$ = 26.04 Å, fixed,
$B = 2b$ = 18.04 Å, fixed,
C, variable (C-axis perpendicular to sheets), α and β, variable, γ = 90°, fixed.

The supercell with Al_{13}^{3+} consists of 6-MMT unit cells, with the same layer composition as for Al_{13}^{5+} $(Al_3Mg_1)Si_8O_{20}(OH)_4$ and the same layer charge density. This supercell (6-MMT) carries the layer charge (6−), balanced with 2 Al_{13}^{3+} cations. In this case, the concentration of cations is 0.33 per MMT unit cell, meaning that the aluminum content after intercalation is 4.33 Al atoms per MMT unit cell. This concentration nearly corresponds to data published by Figueras et al. (1990), where the aluminum content in the interlayer space after intercalation was 4.31 Al atoms per MMT unit cell.

A high concentration of cations, in the case of Al_{13}^{3+}, and presumable interactions between them are required to consider various initial models with different ordering of Keggin cations in the interlayer space. Therefore 2 different shapes of 6-MMT supercell have been taken into consideration. The first 6-MMT supercell (2 × 3-MMT) is:

$A = 2a$ = 10.42 Å, fixed,
$B = 3b$ = 27.06 Å, fixed,
C, variable (C-axis perpendicular to sheets), α and β, variable, γ = 90°, fixed.

The second 6-MMT supercell (3 × 2-MMT) is:

$A = 3a$ = 15.62 Å, fixed,

https://doi.org/10.1346/CCMN.1998.0460302 Published online by Cambridge University Press

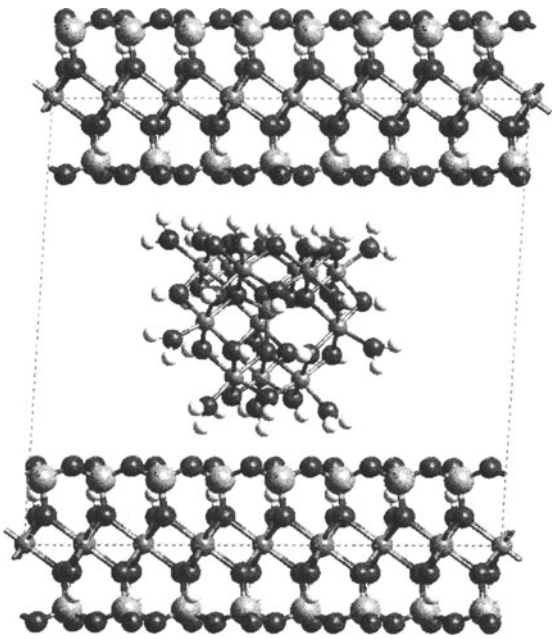

Figure 1. The most stable crystal packing of Keggin cation Al_{13}^{7+} in the 8-MMT supercell. The 3-fold axis of the Keggin-like cation is perpendicular to the silicate layers. Basal spacing $d(001)$ = 19.51 Å.

$B = 2b = 18.04$ Å, fixed,
C, variable (C-axis perpendicular to sheets), α and β, variable, $\gamma = 90°$, fixed.

The Strategy of Energy Minimization using Crystal Packer

The Crystal Packer module in the Cerius[2] modeling environment can be used under the following assumptions: 1) the interactions between the host lattice and intercalant are nonbond and 2) the silicate layers and complex cations can be treated as rigid units, which means that the distortions during intercalation are negligible. The same attitude toward modeling (with rigid clay layers) has been used by Park et al. (1997). In our case, the assumption of rigid units has been supported by 2 different experimental results:

1) Diffraction patterns of intercalated structures were compared with the diffraction pattern of the host structure (Na-montmorillonite). In both cases, the diffraction patterns exhibit the same character, indicating the turbostratic stacking of layers with the typical *hk*-bands. The positions and profiles of *hk*-bands characterizing the lattice parameters *a, b* in silicate layers are exactly the same within the experimental error of ~0.005 Å. That means that the possible contraction or expansion of silicate layers after intercalation should not exceed 0.005 Å.
2) Infrared (IR) spectroscopic measurements were carried out in our laboratory for both samples, intercalated montmorillonite and host structure. The comparison of bands corresponding to the silicate layers in the IR spectrum showed the same positions and profiles of these bands for intercalates and host structures. That means that the possible changes or distortions of Si-O or Al-O bonds must be less than the threshold level of IR detection in the region 1300 to 600 cm^{-1}.

For montmorillonites intercalated by hydroxy-Al species, the bonding between an intercalant and silicate layer is supposed to be ionic (Figueras et al. 1990); therefore, the energy term was set up including the nonbond interactions VDW, COUL and HB. These nonbond interactions are given by the standard well-known expressions, identical in all force fields. The nonbond cutoff distance for the VDW interactions was 7.0 Å, which means that VDW interactions between atoms further apart are ignored. The Ewald sum constant was 0.5 $Å^{-1}$. The minimum charge taken into the Ewald sum was 0.00001 e. All atom pairs with separation less than 10 Å are included in the real-space part of the Ewald sum. All reciprocal-lattice vectors with lengths less than 0.5 $Å^{-1}$ are included in the reciprocal part of the Ewald summation.

In minimizing a very low-density cell, the intermolecular distances may be greater than the nonbond cutoff distance and no attractive interunit forces are calculated. However, by applying an external pressure at the start of minimization, one can bring the rigid units into closer contact. The external pressure of 99 kbar has been applied for the first minimization; then the external pressure was removed and new minimization started.

In the case of the ideal Keggin cation, 2 rigid units have been assigned to the initial model described above: 1) the cation Al_{13}^{7+} and 2) the silicate layer. In supercells 10-MMT and 6-MMT, containing 2 hydrolyzed Keggin cations, 3 rigid units have been introduced: the silicate layer and 2 Keggin cations. (These rigid units could translate and rotate during energy minimization.)

RESULTS

Crystal Packing with Al_{13}^{7+} and Al_{13}^{5+}

The results of energy minimization showed that the crystal packing exhibits certain common features for ideal Al_{13}^{7+} and hydrolyzed Al_{13}^{5+} cations. In both cases, the aluminum and oxygen planes perpendicular to the 3-fold axis of the Keggin cation are oriented parallel to the silicate layers. The resulting model for the 8-MMT supercell with Al_{13}^{7+} is given in Figure 1. Several attempts were made to minimize the initial models with the Al_{13}^{7+} cation strongly tilted with respect to the silicate layer. In all cases, the energy minimization led to the same orientation of Kegin cation described above (Figure 1). Taking into account the shape of the Keggin cation and its concentration (1 cation per one 8-MMT supercell), this resulting model represents the

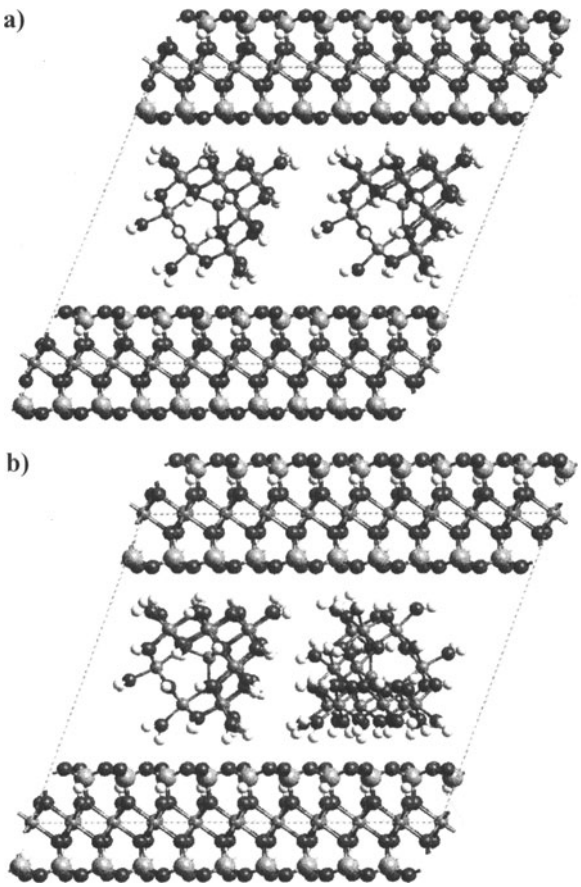

Figure 2. Crystal packing with 2 Al_{13}^{5+} cations in the 10-MMT supercell: a) in parallel arrangement and b) in antiparallel arrangement. Rods and sticks have been used to visualize the positions of atoms in Keggin cations. Basal spacing for both models is 19.60 Å.

closest packing of the intercalated MMT layered structure. Oxygens of the Al_{13}^{7+} adjacent to the silicate layers are bonded via hydrogen bridges to the silicate layer oxygens.

The resulting model for the 10-MMT supercell with 2 Al_{13}^{5+} cations is given in Figure 2. This figure illustrates the packing in the 10-MMT supercell for 2 possible arrangements of Al_{13}^{5+} cations: parallel (a) and antiparallel (b). The results of energy minimization for both arrangements are the same. It is evident from Figure 2 that the orientation of cations Al_{13}^{5+} in the interlayer exhibits the same characteristic features as in case of Al_{13}^{7+}: the oxygen and aluminum planes of Keggin cations are parallel to the silicate layers.

The values of the total sublimation energy (for both 8-MMT and 10-MMT supercells) consisting of VDW, COUL and HB interactions, are presented in Table 1, together with the resulting basal spacings, $d(001)$. As shown in Table 1, coulombic interaction is the dominant part of the sublimation energy in all cases. Due to the higher concentration of Keggin cations and,

Table 1. Average values of basal spacings, d, and van der Waals, coulombic, hydrogen bond and total sublimation energy per supercell for various models of montmorillonite intercalated with $Al_{13}^{(7-x)+}$, for $x = 0, 2, 4$.

Keggin cations in supercell	1 × Al_{13}^{7+} 8-MMT	2 × Al_{13}^{5+} 10-MMT	2 × Al_{13}^{3+} 3 × 2-MMT	2 × Al_{13}^{3+} 2 × 3-MMT
d-spacing (Å)	19.51	19.60	19.65	20.27
VDW (kcal/mol)	137.8	233.0	202.8	191.9
COUL (kcal/mol)	2818.6	2322.4	2067.2	2888.4
HB (kcal/mol)	16.0	22.2	17.7	24.7
E_s (kcal/mol)	2972.4	2577.6	2287.7	3105.0

consequently, shorter distances between them, in the case of Al_{13}^{5+}, the electrostatic repulsion forces between Keggin cations become more important for Al_{13}^{5+} than for Al_{13}^{7+}. As a result, the lower total sublimation energy and slightly higher basal spacing have been observed for Al_{13}^{5+} (Table 1).

After the energy minimization with the Al_{13}^{7+} cation placed in the middle of the 8-MMT supercell, the cation was systematically translated along the sheets and the effect of its position on d-spacing and on the sublimation energy was investigated. The translations of Al_{13}^{7+} were performed in the range of ±2 Å (with the 0.5-Å step) in the B and C directions from its first equilibrium position. In every step, the total sublimation energy was minimized. During these translations, the d-spacing fluctuated within the range of 19.38–19.64 Å. The corresponding fluctuations for all energy contributions were as follows:

VDW in the range of −136.6 to −141.8 kcal/mol,
COUL in the range of −2699.7 to −2877.4 kcal/mol,
HB in the range of −10.5 to −18.9 kcal/mol,
E_s (total sublimation energy) in the range of −2852.0 to −3034.1 kcal/mol.

The average values of d-spacing, VDW, COUL, HB and the total sublimation energy per supercell calculated from these data are presented in the first column of Table 1. As follows from these results, the translation of Keggin cations along the silicate layer does not bring significant changes in d-spacing, coulombic and total sublimation energy per supercell. The relatively large changes of HB energy are due to the fluctuating number of hydrogen bridges involved into the binding forces during translations of Al_{13}^{7+}. The same results have been obtained for translations of Al_{13}^{5+}, respective to Al_{13}^{3+} cations. As both structures, Keggin cations and silicate layers are incommensurate, no correlations can be observed between the $Al_{13}^{(7-x)+}$ position and values of VDW, COUL, HB and d-spacing. As follows from the present results, there is no preference for the XY position of the $Al_{13}^{(7-x)+}$ cation in the interlayer. Therefore, no 2-dimensional ordering of Keggin cations and consequently no regular stacking of layers can be expected in the intercalated montmorillonites. This result is in agreement with the XRD diagrams

https://doi.org/10.1346/CCMN.1998.0460302 Published online by Cambridge University Press

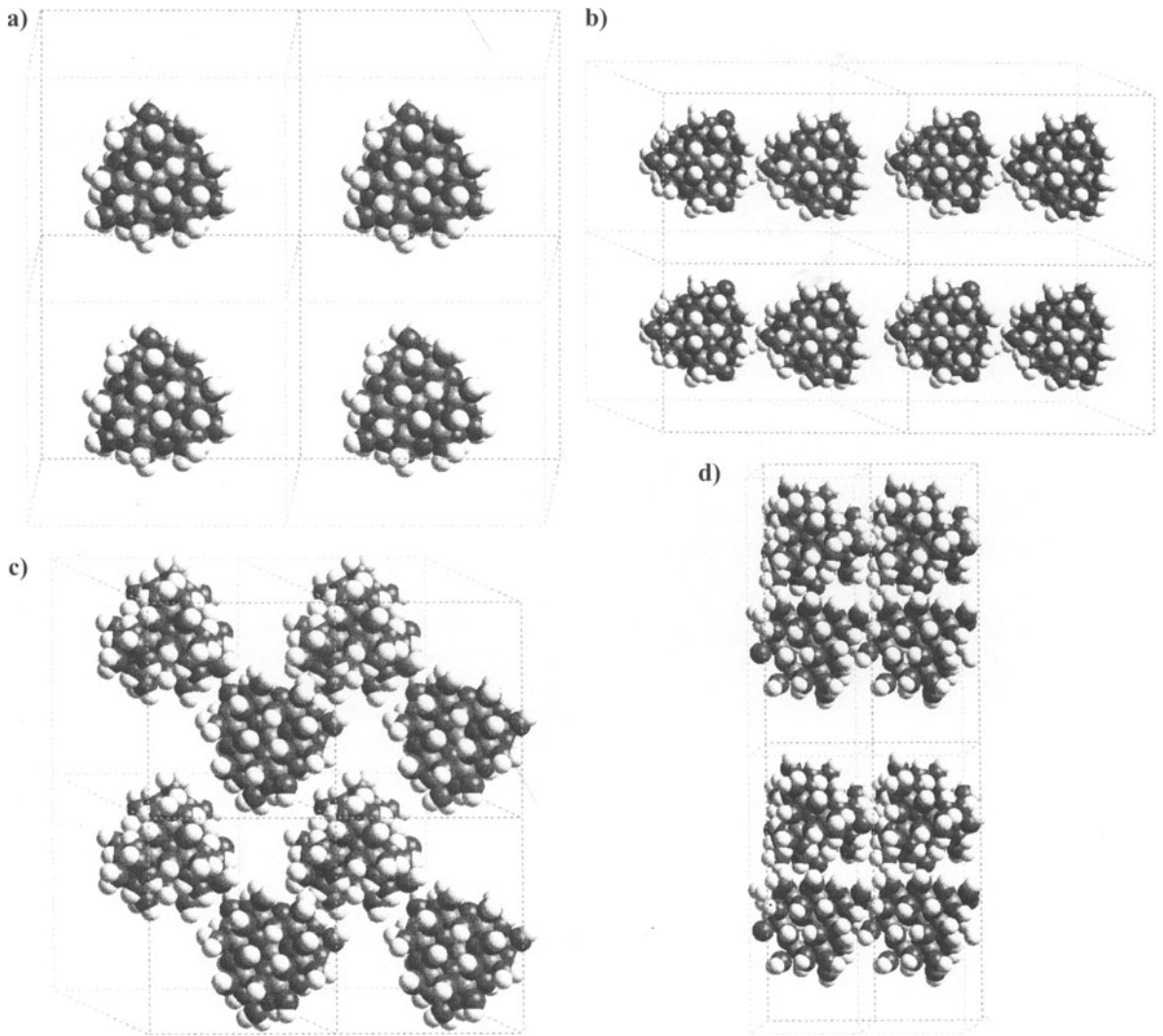

Figure 3. Quadruple supercells for all models used in the present work: a) 4 × 8-MMT supercell, b) 4 × 10-MMT supercell, c) 4 × (3 × 2)-MMT supercell, d) 4 × (2 × 3)-MMT supercell. The silicate layers were removed to illustrate the porosity of the interlayer space (in projection into the plane of sheets).

presented in the literature for intercalated smectites (Zhao et al. 1993).

The effect of layer charge distribution on *d*-spacing and, consequently, on the pore size, has been investigated by rearrangement of Mg atoms in the 8-MMT supercell with Al_{13}^{7+}. For this purpose, the regular distribution of Mg atoms in the supercell was rearranged to the disordered state, with a higher Mg density in the middle and a lower density at the edge of the supercell. The *d*-spacings and energy values obtained after minimization, in the case of disordered Mg atoms, lay in the intervals presented above for the 8-MMT supercell with the ordered Mg atoms. That means that the layer charge inhomogeneity does not influence the sublimation energy and *d*-spacing significantly, which is understandable with respect to the dimensions of Keggin cations.

Crystal Packing with Al_{13}^{3+} Cations

The behavior of the strongly hydrolyzed cations Al_{13}^{3+} in the interlayer space is more complicated than in the previous 2 cases. High concentration of Al_{13}^{3+} cations brings them to closer contact, and their ordering in the interlayer space significantly affects the sublimation energy and the basal spacing. Two extreme cases of ordering are presented in 2 different 6-MMT supercells:

In the 3 × 2-MMT supercell, the distribution of Al_{13}^{3+} cations is homogeneous in the *AB* plane, as shown in Figure 3c. The crystal packing in this case

https://doi.org/10.1346/CCMN.1998.0460302 Published online by Cambridge University Press

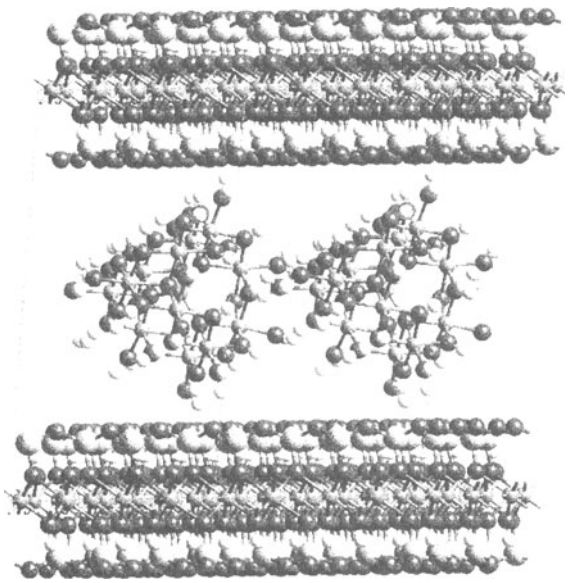

Figure 4. Crystal packing with 2 Al_{13}^{3+} in 2 × 3-MMT supercell. This is the case of the largest basal spacing, 20.27 Å, obtained for models with a different initial rotation of Al_{13}^{3+} cations in the 2 × 3-MMT supercell. For the transparency, only a fragment of the structure is presented in this figure. Two Al_{13}^{3+} cations are shown in the direction of highest density, *A* (see Figure 3d).

is very similar to that of Al_{13}^{7+} and Al_{13}^{5+}, with the Al- and O-planes parallel or almost parallel to the silicate layers. Basal spacing d = 19.65 Å in this case is also near to the d-values for Al_{13}^{7+} and Al_{13}^{5+}. The calculated values of energy are summarized in the third column of Table 1. Because of a higher concentration of Keggin cations in the interlayer, the repulsion forces between them become more important. As a result, the lowest total sublimation energy per supercell obtained in this case shows the weakest Keggin-layer bonding.

In the 2 × 3-MMT supercell, the Al_{13}^{3+} cations are forced to be in very close contact in the *A* direction, where the distances of central aluminum atoms are 10.416 Å. There is more space between them in the *B* direction (Figure 3d). The results of energy minimization for this supercell differ from the previous case (3 × 2-MMT), as shown in Figure 4 and in the last 2 columns of Table 1. In the case of the 2 × 3-MMT supercell with close contact of Al_{13}^{3+} cations, the absolute value of sublimation energy is surprisingly higher than for homogeneously distributed Keggin cations in supercell 3 × 2-MMT. This is caused by stronger Keggin–Keggin coulombic interaction, where the attractive forces between Keggin cations are accompanied by a change of their orientation with respect to silicate layers (Figure 4), resulting in higher basal spacing. The inclination angle of Keggin cations and, consequently, the basal spacing depends on their mutual position (that is, on their rotation around their 3-fold axis). Energy minimization for models with different rotation of cations around the 3-fold axis led to the range of basal spacings 19.80–20.27 Å. The average value d = 20.05 Å is presented in Table 1, together with corresponding average values of VDW, COUL, HB and energy.

The results of modeling showed that proceeding from the homogeneous distribution of Al_{13}^{3+} cations in the 3 × 2-MMT supercell (Figure 3c) to the distribution in the 2 × 3-MMT supercell (Figure 3d), the value of basal spacing varies from 19.65 to 20.27 Å.

Porosity in the Interlayer Space

The small changes of total sublimation energy found during the Keggin translations along the silicate layers showed that there are no special preferences for its positions on these layers. That means no 2-dimensional ordering of $Al_{13}^{(7-x)+}$ cations in the interlayer space and, consequently, no regular distribution of pores respective to channels in the interlayer can occur. The results also showed that Keggin cations can be in very close contact in the interlayer, which means that the interaction forces between $Al_{13}^{(7-x)+}$ cations, depending on their mutual orientation, do not guarantee a minimum pore size, convenient for possible sorption of large organic molecules.

In spite of the irregularity of $Al_{13}^{(7-x)+}$ distribution in the interlayer, we tried to illustrate the Keggin/pores volume ratio in dependence on the degree of hydrolysis. For this purpose, we created quadruple supercells for all of the model analyzed herein. Figures 3a through 3d show these quadruple supercells in the projection to the *AB* plane, where the silicate layers were removed for the transparency. As shown in Figure 3a, the 8-MMT supercell with 1 cation Al_{13}^{7+} exhibits the highest interlayer porosity and lowest basal spacing (d = 19.51 Å). On the other hand, the highest concentration of cations and, consequently, the lowest interlayer porosity, in the case of 2 Al_{13}^{3+} in the 6-MMT supercell, shows the large range of basal spacings, 19.65–20.27 Å, in dependence on their arrangement (Figures 3c and 3d). It is evident from the present results that the value of basal spacing does not represent a reliable parameter characterizing the porosity of structure.

DISCUSSION AND CONCLUSIONS

In molecular mechanics, the energy expression is the basis of all calculations, and its setup involves specifying a number of variables and model parameters. To make the calculations feasible for large molecules, the reasonable cutoff distances have to be introduced to limit the number of pairwise interactions. The results of molecular simulations should be processed keeping in mind all of the approximations accepted in calculations. Therefore, confrontation of the calculated structure model with the experiment is very important, even if there are few experimental data

https://doi.org/10.1346/CCMN.1998.0460302 Published online by Cambridge University Press

available. The present results are in agreement with the experimental data available for intercalated smectites, in 2 main features:

1) in the absence of Keggin cation ordering in the interlayer and, consequently, in the turbostratic stacking of layers (examples of measured diffraction pattern in Zhao et al. 1993 and Plee et al. 1987);
2) in the values of basal spacings.

However, the comparison of basal spacings calculated in the present work with experimental values is complicated, as the range of experimental d-values published by different authors is very wide. This wide variance may be the result of the modulation of diffraction profiles with the steep course of the structure factor, as a function of the diffraction angle. This effect, first described by Reynolds (1980), can lead to a significant shift of peak maximum in dependence on the diffraction angle, peak width and course of structure factor. According to our preliminary calculations, in the case of hydroxy-Al intercalated smectites this effect may lead to the lower basal spacings estimated from the uncorrected diffraction data. The decrease of basal spacing caused by this effect depends on the full width at half maximum (FWHM); for full width at half maximum (FWHM) ~1.4°, we get $\Delta d(001)$ ~1.5 Å. Consequently, authors presenting broader diffraction profiles usually detect basal spacings lower than 19 Å (Plee et al. 1987; Zhao et al. 1993). The values of basal spacings between 19–20 Å are reported by Hsu (1992) and Figueras et al. (1990), who presented relatively sharp diffraction profiles, probably due to better homogeneity of Keggin cations distribution. Taking into account all of the facts mentioned above, we can conclude that the basal spacings obtained in the present work are in agreement with the experiment.

In conclusion, our main results can be summarized as follows:

1) The main contribution to the total sublimation energy comes from the electrostatic interactions. Comparing the values of coulombic energy per Keggin cation (that means for supercells 10-MMT and 6-MMT, the values in Table 1 should be divided by 2), we can see the strongest Keggin-layer binding for Al_{13}^{7+}. For hydrolyzed cations, the distances between them decrease with increasing degree of hydrolysis, and mutual coulombic interactions between them become more important. In the case of Al_{13}^{3+} arranged in the 2 × 3-MMT supercell, the strong electrostatic interactions between them lead to the change of Keggin orientation with respect to layers, resulting in higher basal spacing for strongly hydrolyzed cations (Figure 4).
2) A relatively wide range of basal spacings has been found: from 19.38 Å for Al_{13}^{7+} to 20.27 Å for Al_{13}^{3+} arranged in the 2 × 3-MMT supercell. That means that when the real sample of $Al_{13}^{(7-x)+}$ intercalated montmorillonite contains Keggin cations in different degrees of hydrolysis, one can expect inhomogeneity in basal spacings, leading to the corresponding broadening of diffraction profile 001.
3) Translation of Keggin cations along the silicate layer does not bring significant changes in d-spacing, coulombic and total sublimation energy. That means that there is no significant preference for the position (XY coordinates) of $Al_{13}^{(7-x)+}$ cations in the interlayer. As a result, no 2-dimensional ordering of $Al_{13}^{(7-x)+}$ cations in the interlayer and no regular stacking of layers can be expected in the intercalated montmorillonites.
4) In pillaring clays, the main aim is to achieve as large a basal spacing as possible according to the widely accepted opinion that large basal spacings give rise to a large volume of pores. The present results, however, showed that the relation between basal spacing and porosity can be more complicated. Porosity is more likely ruled by the charge of Keggin cations. The value of basal spacing may be misleading in characterizing porosity in montmorillonites intercalated with Keggin cations.

REFERENCES

Driessen RAJ, Loopstra BO, de Bruijn DP, Kuipers HPCE, Schenk H. 1988. Program PLUVA. J Computer-Aided Molecular Design 2:225–240.
Figueras F. 1988. Pillared clays as catalysts. Catal Rev Sci Eng 30:457–499.
Figueras F, Klapyta Z, Massiani P, Mountassir Z, Tichit D, Fajula F. 1990. Use of competitive ion exchange for intercalation of montmorillonite with hydroxy-aluminum species. Clays Clay Miner 38:257–264.
Hsu PH. 1992. Reaction of OH-Al polymers with smectites and vermiculites. Clays Clay Miner 40:300–305.
Johansson G. 1960. On the crystal structure of some basic aluminium salts. Acta Chem Scand 14:771–773.
Malla PB, Komarneni S. 1993. Properties and characterization of Al_2O_3 and SiO_2-TiO_2 pillared saponite. Clays Clay Miner 41:472–483.
Mayo LS, Olafson BD, Goddard WA III. 1990. DREIDING: A generic force field for molecular simulations. J Phys Chem 94:8897–8909.
Mering J, Oberlin A. 1967. Electron-optical study of smectites. Clays Clay Miner 27:3–18.
Occelli ML, Rennard RJ. 1988. Hydrotreating catalysts containing pillared clays. Catal Today 2:309–319.
Park S, Fitch A, Wang Y. 1997. Computational studies compared to electrochemical measurements of intercalation of cationic compounds in Wyoming montmorillonite. J Phys Chem 101B:4889–4896.
Pinnavaia TJ, Tzou MS, Landau SD, Raythatha RH. 1984. On the pillaring and delamination of smectite clay catalyst by polyoxo-cations of aluminum. J Mol Catal 27:195–212.
Plee D, Borg F, Gatineau L, Fripiat JJ. 1985. High resolution solid-state ^{27}Al and ^{29}Si nuclear magnetic resonance study of pillared clays. J Am Chem Soc 107:2362–2369.
Plee D, Gatineau L, Fripiat JJ. 1987. Pillaring processes of smectites with and without tetrahedral substitution. Clays Clay Miner 35:81–88.
Reynolds RC, Jr. 1980. Crystal structure of clay minerals and their X-ray identification. Brindley GW, Brown G, editors. London: Mineral Soc. p 249–303.

Schoonheydt RA, Leeman H, Scorpion A, Lenotte I, Grobet P. 1994. The Al pillaring of clays. Part II. Pillaring with $[Al_{13}O_4(OH)_{24}(H_2O)_{12}]^{7+}$. Clays Clay Miner 42:518–525.

Sterte J. 1991. Preparation and properties of large-pore La-Al-pillared montmorillonite. Clays Clay Miner 39:167–173.

Tichit D, Fajula F, Figueras F, Ducourant B, Mascherpa G, Gueguen G, Bousquet J. 1988. Sintering of montmorillonites pillared by hydroxy-aluminum species. Clays Clay Miner 36:369–375.

Tsipursky SI, Drits VA. 1984. The distribution of octahedral cations in 2:1 layers of dioctahedral smectites studied by oblique-texture electron diffraction. Clay Miner 19:177–193.

Zhao D, Wang G, Yang Y, Guo X, Wang Q, Ren J. 1993. Preparation and characterization of hydroxy-FeAl pillared clays. Clays Clay Miner 41:317–327.

(Received 29 May 1996; accepted 9 August 1997; Ms. 2778, Part I)